Journal of the Serbian Chemical Society
JSCS-info@shd.org.rs • www.shd.org.rs/JSCS

ACCEPTED MANUSCRIPT

Please cite this article as F. Mustafayeva, and N. Kakhramanov, *J. Serb. Chem. Soc.* (2026) https://doi.org/10.2298/JSC260426039M

Journal of the Serbian Chemical Society
JSCS-info@shd.org.rs • www.shd.org.rs/JSCS
J. Serb. Chem. Soc. **00(0)** 1-18 (2026)
JSCS–13932
Original scientific paper
Published DD MM, 2026

Advanced polypropylene random copolymer nanocomposites: effect of natural bentonite clay and aluminum hydroxide on morphology and properties

FATIMA MUSTAFAYEVA[1,2]*, AND NAJAF KAKHRAMANOV[1]

[1]*Institute of Polymer Materials of Ministry of Science and Education Republic of Azerbaijan, Sumgayit city, S. Vurgun Str. 124, AZ5004, Azerbaijan, and* [2]*Sumgayit State University, Sumgayit city, 43rd district, Baku street 1, AZ5008, Azerbaijan.*

(Received 26 April; revised 20 June; accepted 23 July 2026)

Abstract: This paper examines the influence of nanoparticles of the natural mineral bentonite and aluminum hydroxide on the obtain of nanocomposites based on a compatibilized polypropylene random copolymer. A random copolymer of ethylene and propylene modified with maleic anhydride was used as a compatibilizer. The total amount of filler introduced into the polypropylene random copolymer composition was 50 wt.%. To study the synergistic effect when using a mixture of fillers, bentonite was included in the formulation at five different concentrations (5, 10, 15, 20 and 25 wt.%). The composites were obtained by mechanical mixing in the melt of a compatibilized polymer matrix. The structural, morphological, physical-mechanical, thermal properties and fire resistance of the obtained composite materials were determined. The structural and morphological properties were characterized using infrared spectroscopy (IR) and scanning electron microscopy. Based on the results of IR spectroscopy and Scanning Electron Microscopy-Energy Dispersive X-ray Spectroscopy (SEM-EDX) spectra, the presence of elements and bonds corresponding to the composition of bentonite and aluminum hydroxide, which were used as fillers in the composition of the polypropylene random copolymer, was confirmed. Morphological study revealed minor agglomerates of bentonite nanoparticles. Thermal properties of the obtained composites were determined using thermogravimetric analysis and differential scanning calorimetry. Thermogravimetric analysis showed that the addition of bentonite increases the thermal stability of composites, as evidenced by a decrease in the rate of mass loss. Mechanical properties (tensile strength, elongation at break) decrease with increasing bentonite concentration. The synergistic effect obtained by the combined use of aluminum hydroxide and bentonite was manifested mainly in an increase in the melt flow index of the composite. The sample containing 25

* Corresponding author. E-mail: mustafayevafatima@mail.ru, fatime.mustafayeva@sdu.edu.az
https://doi.org/10.2298/JSC260426039M

wt. % natural bentonite showed the highest melt flow index values, up to 3.12 g/10 min.

Keywords: polypropylene random copolymer; bentonite; aluminium hydroxide; physical and mechanical properties; melt flow index; surface morphological properties; thermal properties; thermomechanical properties..

INTRODUCTION

Improving the performance properties of polymer composite materials is one of the current areas in the field of materials science. When developing a recipe, it is necessary to improve the physical and mechanical properties while maintaining technological effectiveness. One of the most promising approaches to the creation of polymer composites is the use of bifunctional layered silicates as polymer fillers. The main attractive feature of bentonite clay-polymer composites is that small amounts of nanoclay can be used to enhance the functional properties of the polymer without compromising other key characteristics. Bentonite, as an inorganic mineral whose main component is montmorillonite, has advantages such as large deposits in Azerbaijan, availability and low cost. The introduction of cheap minerals into the polymer composition helps to significantly reduce the cost of the composite material. A number of studies[1-3] have reported on the influence of bentonite on the structure and properties of various polymers. However, individual fragmentary information on the modification of the properties of polyolefins by bentonite does not allow us to systematize the research into a single, comprehensive theory. This is especially true for research in the field of developing fire-resistant materials. It is known that bentonite and montmorillonite belong to the group of clay minerals, distinguished by a unique combination of a layered structure with high flame retardancy.[4] In the process of studying the influence of structural features of layered silicates on the combustion process of polymer composites, 2 mechanisms for reducing flammability were proposed.[5] The first mechanism consisted of the formation of a carbonized layer, which affected the mass and heat transfer between the combustion zone and the polymer material. The second mechanism was based on the possible catalytic activity of aluminosilicates in the process of thermal destruction of the polymer. Also, it is necessary to take into account the fact that bentonite, at a certain content in the composition of the composite, can contribute to the improvement of their basic strength properties, in particular, tensile strength, bending strength and impact strength.[6,7] This is due to the ability of bentonite, as a filler-reinforcer, to act as a reinforcing agent, improving the overall mechanical characteristics of the composite.[8,9]

Metal hydroxides are effective flame retardants that improve the environmental performance of fire-resistant composites. These flame retardants account for 40% of the total polymer flame retardant materials market by weight.[10] Their flame retardancy is due to strong endothermic decomposition with the

release of water. Aluminum hydroxide is a flame retardant that is widely used in various types of polymers due to its ability to suppress smoke and prevent the spread of fire.[11] When introduced into the polymer matrix, aluminum hydroxide performs two main functions. It acts as a filler, as well as a flame retardant and smoke suppressant. For effective action, the recommended loading of aluminum hydroxide in the polymer composite is 40–65 wt.%.[12–14] However, to achieve a satisfactory fire protection effect, a large amount of aluminum hydroxide is required, which to a certain extent negatively affects the physical, mechanical and operational properties.

Yand et al. in their work[15,16] showed that the addition of a mixture of aluminum hydroxide with organic montmorillonite slows down the thermal decomposition of the polymer composite and shows good thermal insulation properties, while reducing heat release during combustion. Kaleg et al. found that the addition of aluminum hydroxide and montmorillonite did not result in significant changes in the decomposition temperature of unsaturated polyester, but tended to decrease the maximum mass loss rate.[17] Based on the above ideas, we proposed a convenient strategy to replace part of the aluminum hydroxide with bentonite in a compatibilized polypropylene random copolymer.

Overall, this work allows for a simple and environmentally friendly green approach to using Azerbaijan's natural mineral resources in conjunction with flame retardants. In particular, this work examined the combined use of aluminum hydroxide with bentonite clay for use as a multifunctional flame retardant system. For this purpose, a study was conducted on the influence of different ratios of aluminum hydroxide to bentonite on the structural, morphological, physical-mechanical, thermal and fire-resistant properties of the obtained composites. The following composition was used as the base composition: polypropylene random copolymer / compatibilizer / aluminum hydroxide with a component ratio (wt.%) of 47/3/50.

EXPERIMENTAL

Materials

The properties of the polymer-based components used in the studies are presented in Table I.

Concentration of fillers was fixed at 50 wt. % of total amount of composite. The fillers used in studies differ in shape and size. To prepare to polymer composites aluminum hydroxide with particle sizes Dv(10) = 0.0197 μm, Dv(50) = 0.0559 μm, Dv(90) = 0.159 μm were used (Fig. 1) .

TABLE I. Properties of polymer matrix and compatibilizer

	Name	Brand	Manufacturer	Melt flow index	Melting temp (°C)
Polymer	Polypropylene random copolymer – PP-R	Topilene® R200P	Hyosung Chemıcal Corporatıon	0.2 g/10 min (230 °C, 2.16 kg)	145
Compatibiliser	Polypropylene copolymer grafted with maleic anhydride – PPC-g-MAH	DuPont™ Fusabond® P353	DuPont Company	470 g/10 min (190 °C, 2.16 kg)	135

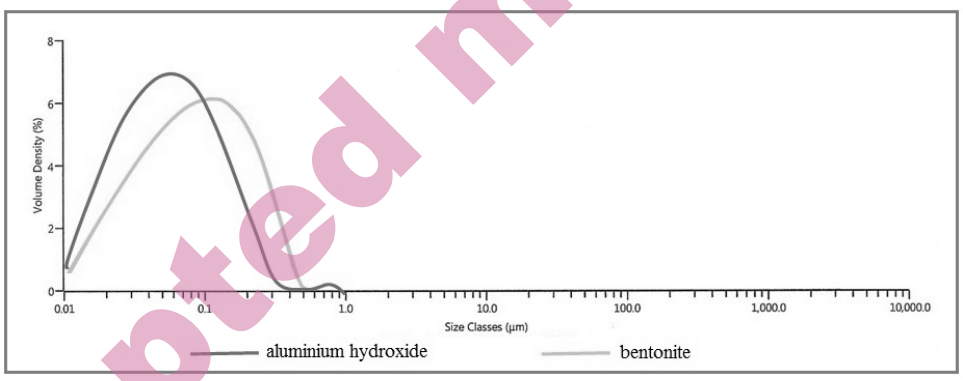

Fig. 1. Particle size of fillers

The dosage of bentonite (origin of the Dash-Salahli deposit of the Azerbaijan Republic) varied in the range of 0-25 wt. %. The oriented particle size of the bentonite used is generally less than 0.248 µm: Dv(10) = 0.024 µm, Dv(50) = 0.0855 µm, Dv(90) = 0.248 µm. The Analytical Center of the Institute of Geology and Geophysics of the Ministry of Science and Education of the Republic of Azerbaijan determined the bentonites mineralogical (XRD Miniflex 600, Rigaku, Japan) and chemical (XRF S8 Tiger, Bruker, Germany) composition (Table II and III).

TABLE II. Chemical composition of bentonite (in %)

Na_2O	MgO	Al_2O_3	SiO_2	P_2O_5	SO_3	K_2O	CaO
1.61	2.00	12.57	58.71	0.22	0.10	2.70	8.05
TiO_2	MnO	Fe_2O_3	BaO	SrO	V_2O_5	Cl^-	
1.11	0.14	8.83	0.002	0.07	0.02	0.02	

the amount of volatile components at 950 °C temperature – 0.83

TABLE III. Mineralogical composition of bentonite (in %)

SiO_2 (α quartz)	Anorthite	Montmorillonite	Vesuvianite	Clinoptilolite
10	25	57	0	0
Lamontite	Fe_2O_3 (hematite)	Fe_3O_4 (magnetite)	Amorphous	Other mixtures
0	8	0	0	0

Sample preparation

The polymer composite samples based on PP-R/PPC-*g*-MAH/$Al(OH)_3$/bentonite were prepared in three stages. The first stage involved the preparation of polymer composites using a twin-roll mixer at a temperature of 170°C. The mixing time was 8–10 minutes and the rotor speed was 50 rpm. The mixing of components was carried out in stages. PPC-*g*-MAH was added to the PP-R melt, followed by fillers. At the second stage, the materials extracted from the rolls were pressed at a temperature of 190 °C. The third stage involved cutting out blade samples from the pressed plates to test their strength characteristics. Table IV shows the formulations used and sample identification. The numbers in the sample designations indicate the content of the filler used. Using the mechanical melt mixing method, composite formulations were prepared using two fillers, as shown in Table IV.

TABLE IV. Identification and formulations of all prepared samples

Sample code	PP-R (wt.%)	PPC-*g*-MAH (wt.%)	$Al(OH)_3$ (wt.%)	Bentonite (wt.%)
$AH_{45}Bt_5$	47	3	45	5
$AH_{40}Bt_{10}$	47	3	40	10
$AH_{35}Bt_{15}$	47	3	35	15
$AH_{30}Bt_{20}$	47	3	30	20
$AH_{25}Bt_{25}$	47	3	25	25

Characterization methods

Fourier transform infrared spectroscopy (FTIR)

An Agilent Cary 630 FTIR device from Agilent Technologies (India) was used to record the samples infrared spectra. Every spectrum was gathered between 4000 and 600 cm^{-1} in wavenumber.

Scanning electron microscopy (SEM) analysis

A scanning electron microscope, model JSM-6610 (JEOL, Japan), was used to investigate the surface morphology of the composites.

Particle size analysis

A Mastersizer 3000 laser analyzer from Malvern Instruments (England) used to measure the particle size of fillers (bentonite, aluminum hydroxide). The range of operation was 0.1 to 3500 microns. Measurements were made in distilled water.

Melt flow index

The CEAST MF50 branded Melt Flow Tester (INSTRON company, Italy) was used to evaluate the melt flow index (MFI) of the filled PP-R composites in accordance with ASTM D1238. The length and diameter of the capillary were 8 mm and 2.095 mm, respectively. With

a preheating period of 10 minute and a 5 kg weight, the temperature was 190 °C. Four every sample, four replicate measurements were made.

Physical and mechanical properties

Using a WPM, VEB, Thuringer industriewerk, Rauenstein R-40, TYP-2092 tensile testing machine in accordance with GOST 11262-80 (ASTM D 638), the physical and mechanical characteristics of the polymer composite materials were investigated at a speed of 50 mm/min movable grips of (four samples were tested). This study presents the average tensile strength value of the four specimens for each composite.

Thermal analysis

Thermal analysis: The thermal characteristics, decomposition process, and thermal stability of the composites were ascertained using Thermogravimetric Analysis (TGA), Differential Scanning Calorimetry (DSC) and Differential Thermogravimetric Analysis (DTG). A Perkin Elmer STA 6000 Simultaneous Thermal Analyzer was used for measurements. A nitrogen atmosphere was used to scan the sample weight of approximately10 mg between 25.00 to 750.00 °C at a heating rate of 10.00 °C/ min.

A Kanavets device was used to ascertain the samples thermomechanical characteristics. With a load of 0.5 kg/cm^2 and a heating rate of 50 °C/h, the deformation was recorded at sequentially varying temperatures (T). Tables with a flat surface that were 24 mm in diameter, 6 mm high and weighed 3.5-4 g were pressed into a special mold in order to conduct research. Thermomechanical curves $\Delta = f(T)$ showing the dependence of polymer composites were created using experimental data.

Resistance to burning

ASTM D3801 (Standard Test Method for Measuring the Comparative Burning Characteristics of Solid Plastics in a Vertical Position) was used for conducting fire resistance investigations of polymer composite products.

RESULTS AND DISCUSSION

PPC-*g*-MAH increases the polarity of polypropylene random copolymer. The presence of a compatibilizer in the non-polar polymer matrix promotes adhesive interactions between the incompatible dispersed and dispersion phases. FTIR analysis reveals possible structural information and examines the bond interaction between all components in the composite system. Fig. 2 shows the FTIR spectra of PP-R/PPC-g-MAH/Al(OH)$_3$/bentonite composites.

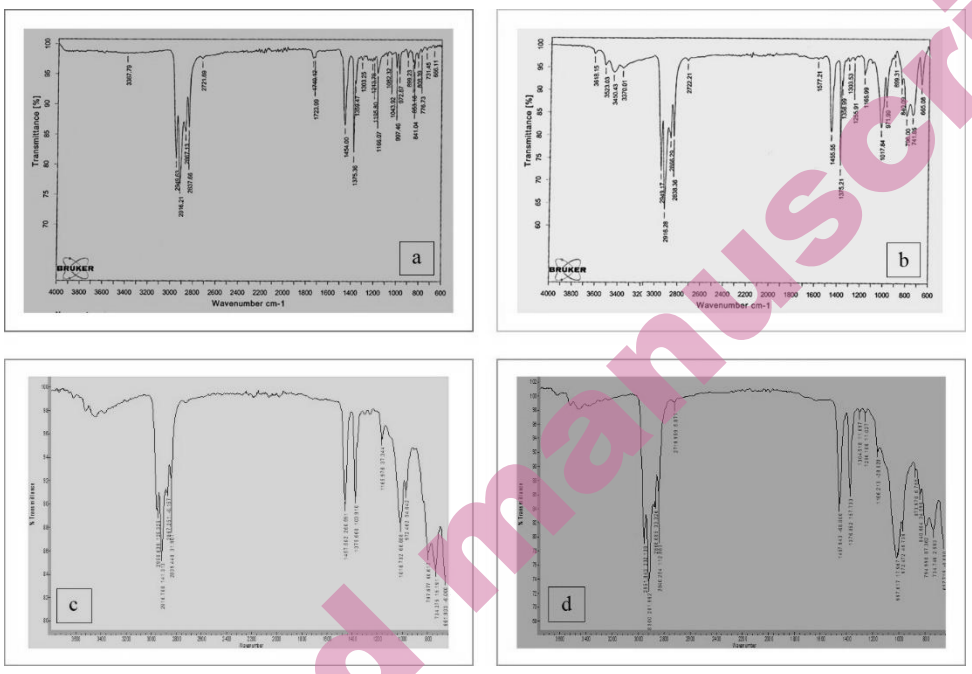

Fig. 2. IR spectra of PP-R (a), PP-R/PPC-*g*-MAH/50 wt. % $Al(OH)_3$ (b), $AH_{45}Bt_5$ (c) and $AH_{25}Bt_{25}$ (d) polymer composites

The characteristic absorption bands observed across the FTIR spectra correspond directly to the functional groups of the polymer matrix (PP-R), the compatibilizer (PPC-g-MAH), and the inorganic fillers ($Al(OH)_3$ and bentonite clay). Matrix and compatibilizer bands (present in all spectra): 2950 – 2840 cm^{-1} intense, sharp peaks originating from the asymmetric symmetric C – H stretching vibrations of – CH_3 and – CH_2 – groups in the PP-R backbone; 1450 – 1460 cm^{-1} medium peak corresonding to C – H bending deformations of – CH_3 and – CH_2 – groups; 1375 – 1380 cm^{-1} sharp peak assigned to the – CH_3 umbrella mode (symmetric bendix vibration of methyl side chains), a classic fingerprint for polypropylene; 1730 – 1750 cm^{-1} (spectra b, c, d) a distinctive C = O carbonyl stretching vibration band introduced by the PPC – g – MAH compatibilizer (grafted maleic anhydride groups).

Aluminum hydroxide absorption bands (spectra b, c, d): 3620 – 3300 cm^{-1} a series of strong, sharp peaks (visible at approximately 3619, 3523, 3450 and 3393 cm^{-1}) representing the crystalline intermolecular and intramolecular O – H stretching vibrations of the gibbsite ($Al(OH)_3$) structure; 1020 – 960 cm^{-1} enhanced absorption intensity caused by the Al – OH bending / deformation modes.

As the concentration of bentonite increases from 5 wt. % (c) to 25 wt. % (d), several distrinct aluminosilicate silicate bands appear and intensify. Bentonite clay

absorption bands (spectra c and d): 1030 – 1050 cm^{-1} a massive, broad peak that progressively dominates the fingerprint region. It originates from the Si – O – Si in plane asymetric stretching vibrations of the tetrahedral clay layers; 3620 cm^{-1} overlaps with $Al(OH)_3$ peaks, corresponding to the structural hydroxyl stretching within the clay lattice; 520 cm^{-1} and 460 cm^{-1} prominent bands at lowest frequency range representing Al – O – Si stretching and Si – O – Si bending vibrations of the clay framework.

The appearances of all characteristic peaks were correlated to the distribution and dispersion of inorganic fillers in the composites. It can be confirmed from the FTIR spectroscopy that the functional groups, which were present in the individual materials had their influence in the composite formation and no new peaks were found indicating no additional functional groups were formed. The IR spectrum of composite show characteristic band of both the PP-R and bentonite which ensures the incorporation of clay in the polymer. Referring to spectra of bentonite filled composites in comparison to the PP-R/PPC-*g*-MAH/50 wt. % $Al(OH)_3$, it was found that all spectra were very close to each another. However, the presence of bentonite caused slight changes in the position and intensity of the aborption band. Moreover, the intensities of peak related to the Si-O-Si stretching band, were more pronounced, which characterizes the presence of bentonite in the composites.

It is known that the supramolecular structure of a composite predetermines its final properties. The dispersion state of bentonite in the PP-R/PPC-*g*-MAH/$Al(OH)_3$ composition was further confirmed by SEM analysis (Fig. 3).

The surface structure of $AH_{45}Bt_5$ and $AH_{25}Bt_{25}$ composites observed via SEM are compared in Fig. 3. Agglomeration morphology of bentonite in some areas due its poor dispersion is noticeable in SEM. The EDX analysis of composites showed the presence of K (potassium), C (carbon), Ca (calcium), O (oxygen), Fe (iron), Na (sodium), Mg (magnesium), Si (silicon) and Al (aluminum) element. The obtained results confirm the fact of obtaining a composite of the composition PP-R, PPH-*g*-MAH, $Al(OH)_3$ and bentonite.

In particular, changes in MFI can be used to judge the structural and rheological changes occurring in the polymer matrix under the influence of various factors. The study of the dependence of the MFI of PP-R/PPC-*g*-MAH/$Al(OH)_3$ on the bentonite content showed that the significantly affects the viscosity of the composite melt. As can be seen from Fig. 4, the replacing of $Al(OH)_3$ with bentonite leads to a fairly sharp increase in the MFI values of the polymer. Obviously, this behavior is associated with structural changes occurring in the polymer matrix. We do not exclude that as a result of thermomechanical action, the layered structure of bentonite decomposes with the release of surface-active substances, including glycerin, which significantly leads to an increase in the MFI of the composites. In general, the MFI values of the obtained PP-R/PPC-*g*-MAH/$Al(OH)_3$/ bentonite composites are higher than those of the PP-R/PPC-*g*-

MAH/50 wt. % $Al(OH)_3$, as well as the MFI values of industrial PP-R. This indicaes that the types/nature, size, quantity and dispersion status of fillers are playing a major role in the properties of the prepared composites more than the number of the used fillers.[18]

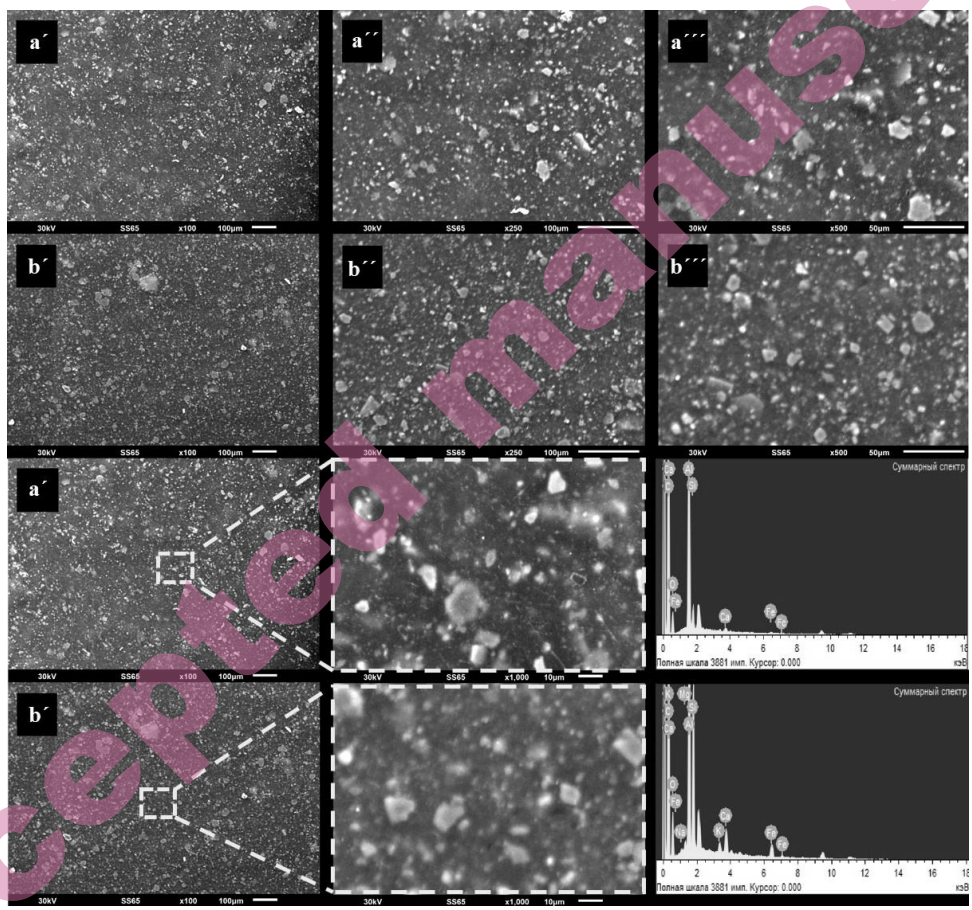

Fig. 3. EDX spectra and SEM images of $AH_{45}Bt_5$ (a) and $AH_{25}Bt_{25}$ (b) polymer composites at different magnifications

Fig. 4 shows the results of studies of the physical and mechanical characteristics of polymer composite materials based on PP-R/PPC-g-MAH/$Al(OH)_3$/bentonite. The obtained results indicate a significant influence of bentonite concentration on physical and mechanical properties. With an increase in the concentration of bentonite, a slight decrease in the mechanical characteristics of the composite was recorded.

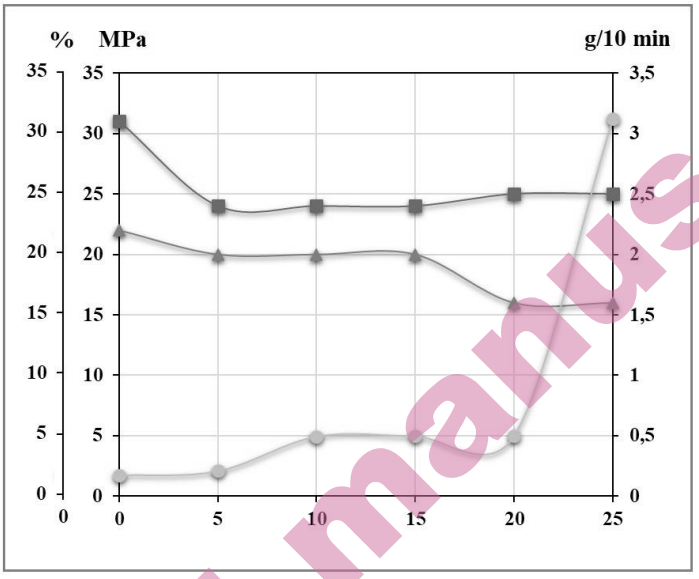

Fig. 4. Physical-mechanical properies of PP-R/PPC-*g*-MAH/$Al(OH)_3$/ bentonite based polymer composites: ▲ – elongation at break, ■ – tensile strength, ● – MFI

Generally, the strength properties of the composite strongly related to the interfacial interaction between the filles and matrices. The specific surface area and particle size resulted in better dispersion of filler. The agglomeration of fillers can be a possible explanation for the reduction of tensile strength at higher filler loading. Refering to Fig. 4, it can be concluded that the tensile strength was decreased with the increase of bentonite concentration from 5 wt. % to 25 wt. %. Agglomeration of fillers may be a possible explanation for the decrease in tensile strength at higher bentonite loading. It is believed that fillers with smaller particle sizes, such as aluminum hydroxide, provide a larger contact area with the polymer matrix due to their higher surface area compared to bentonite. The specific surface area and particle size resulted in better dispersion of the filler. This is most likely why replacing aluminum hydroxide nanoparticles with bentonite resulted in a decrease in strength.

On the other hand, Fig. 4 shows elongation at break of the studied composites. The elongation at break decreased monotonically with increasing bentonite content and decreased by approximately 27 % at a bentonite concentration of 25 wt. %. Poor interaction between $Al(OH)_3$ and bentonite, and with the matrix may have contributed to lower properties in composites.

TGA has been used to evaluate the thermal stability of obtained composites. Generally, inorganic species have good thermal stability. Introduction of inorganic components into organic materials improve the thermal stability of the resulting

composite. The most prominent effect of particulate fillers on the crystalline structure of semi-crystalline thermoplastics is their ability to work as a nucleation agent. Though there has been some debate over the effects of crystalline changes on macromechanical properties, it seems clear that by increasing crystallinity, the strength and deformability of PP-R decrease.

Thermogravimetric curves of both composites have two clearly defined stages of mass loss. The decrease in mass of both composites began above of 240 °C. The thermal weight loss of PP-R/PPC-*g*-MAH/$Al(OH)_3$/ bentonite composites main occured in the range of 240 °C – 450 °C, and the mass loss was about 65 -60 %. A TGA study of the obtained composites showed that their heat resistance depends on the bentonite content. The increase in heat resistance with a low bentonite content is due to intermolecular interactions and the features of the resulting phase structure. The residue obtained at the end of the TGA scan (750 °C) showed a value of approximately 34.181% for the $AH_{45}Bt_5$ composite and 39.076% for the $AH_{25}Bt_{25}$. The increase in solid residue is primarily driven by replacing $Al(OH)_3$ with bentonite. At 750 °C, $Al(OH)_3$ fully decomposes into volatile H_2O and Al_2O_3, while bentonite is highly thermally stable, retaining a greater proportion of its mass to form a denser residual structure. Bentonite is a clay mineral composed of aluminosilicate. It is highly thermally stable and does not degrade or release volatile gases at 750 °C like the polymer or hydroxide do. Thus, an increased bentonite content leads to larger absolute mass of stable inorganic minerals in the final residue.

The thermal properties of PP-R/PPC-*g*-MAH/$Al(OH)_3$/bentonite based composites with different bentonite loading levels were also studied by DSC and the corresponding thermographs are given in Fig. 5. The melting enthalpy ΔH_m and melting temperature T_m obtained from the DSC analysis for $AH_{45}Bt_5$ and $AH_{25}Bt_{25}$ composites were summarized in Table V. The results showed that the melting temperature and melting enthalpy of the composites increased with the increase of bentonite amount. A strong endothermic peak average value around 138.61 °C is visible, which is most likely associated with the melting of the crystalline domains of the $AH_{45}Bt_5$ composite. Double melting peaks can be associated with crystals having different morphology and, accordingly, thermal stability, crystalline perfection or crystallite sizes, polymorphism.[19] The melting peak temperature T_m of PP-R/PPC-*g*-MAH/$Al(OH)_3$/bentonite composites increase with the addition of bentonite. The melting enthalpy (ΔH_m) of PP-R/PPC-*g*-MAH/$Al(OH)_3$/bentonite increased with the addition of bentonite. The increase in melting enthalpy values can be explained by amount of free volume between PP-R chains capable of allowing bentonite to be intermixed.

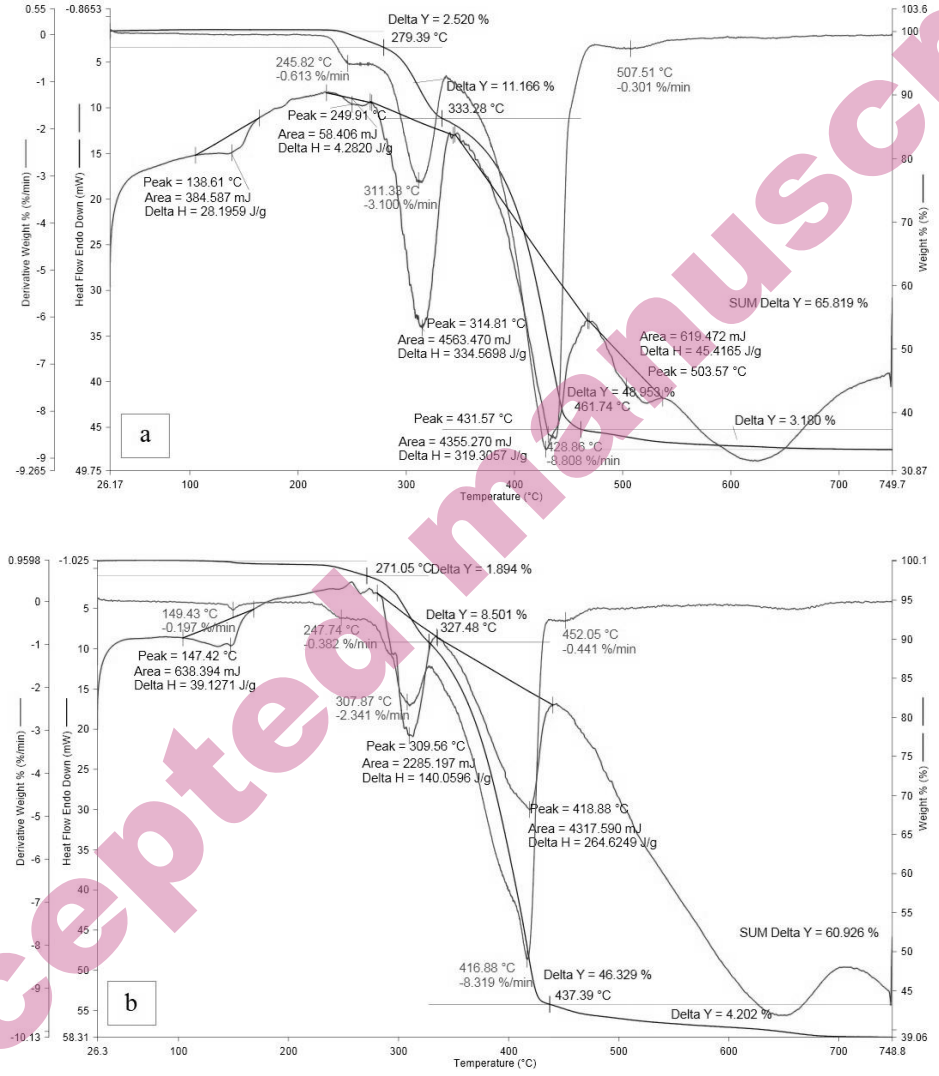

Fig. 5. Thermal analysis results for $AH_{45}Bt_5$ (a) and $AH_{25}Bt_{25}$ (b) polymer composites

The heating thermogram of $AH_{25}Bt_{25}$ shows a single melting endopeak with a maximum at 147.42 °C and an enthalpy of 39.1271 Jg^{-1}. Table V shows the melting enthalpies of composites. The endopeak enthalpy of melting of PP-R / PPC-g-MAH / 50 wt. % $Al(OH)_3$ was 48.2213 Jg^{-1}, while that of PP-R was higher, reaching a value of 56.6878 Jg^{-1}. The melting enthalpy characterizes the energy required to break intermolecular bonds in a crystal during the transition from a solid state to a viscous flow state.[20] In similar PP-R, intermolecular bonds are

determined by the van der Waals interaction energy. The decrease in enthalpy in $AH_{25}Bt_{25}$ indicates a decrease in intermolecular interactions.

TABLE V. Scanning calorimetry data corresponding to $AH_{45}Bt_5$ and $AH_{25}Bt_{25}$ polymer composites

Sample	PP-R	$AH_{45}Bt_5$	$AH_{25}Bt_{25}$
Onset mass loss temperature (°C)	345.32	279.39	271.05
Maximum weight loss rate temperature (°C)	451.48	428.86	416.88
Maximum weight loss rate (%/min)	-25.715	-8.808	-8.319
Solid residue under 750 °C (%)	0.3 (at 700 °C)	34.181	39.076
T_m (°C)	145.36	138.61	147.42
ΔH_m (Jg^{-1})	56.6878	28.1959	39.1271

The thermogram of $AH_{45}Bt_5$ and $AH_{25}Bt_{25}$ has a regular symmetrical shape, which indicates a fairly homogeneous crystalline phase.[21] The enthalpy of melting of $AH_{25}Bt_{25}$ was greater than the enthalpy of melting of $AH_{45}Bt_5$. If in $AH_{25}Bt_{25}$ the enthalpy of melting was only 11 Jg^{-1} higher than the enthalpy of melting of $AH_{45}Bt_5$, then in PP-R the enthalpy was 56 Jg^{-1}. Obviously, this is due to a decrease in the degree of crystallinity of PP-R due to the influence of filler particles on the crystallization process.

A series of experiments with samples of different compositions showed that they all have thermograms of similar shape. The positions of the maximum melting temperature on the temperature scale are shifted relative to the melting temperature of the original PP-R. Based on the DSC data, it can be said that the introduction of 25% bentonite into PP-R leads to an increase in the melting temperature. It has been established that the introduction of 45% $Al(OH)_3$/5% bentonite leads to a decrease in the melting temperature. When interpreting the DSC results, it can be assumed that the increase in the enthalpy of melting of $AH_{25}Bt_{25}$ as a result of the introduction of 25% of the amount of bentonite is due to the fact that bentonite promotes an increase in the number of heterogeneous nucleation centers, which contributes to an increase in the total rate of crystallization of PP-R. An increase in the rate of crystallization from two centers – homogeneous and heterogeneous nucleation centers – leads to the simultaneous formation of many small-sized crystallites, which, as a result of steric limitations during their growth, form a crystalline phase with a minimum number of defects compared to the PP-R crystalline phase.[22]

Similarly, thermomechanical analysis recorded an increase in the softening temperature and viscous flow state of the composites (Fig. 6). By analyzing the thermomechanical curves in Fig. 6, it can be established that the test samples are not subject to deformation over a wide temperature range.[23] According to this method, the melting point of the samples changed in the following sequence: $AH_{25}Bt_{25}$ – 149 °C, $AH_{30}Bt_{20}$ – 145 °C, $AH_{35}Bt_{15}$ – 146 °C, $AH_{40}Bt_{10}$ – 153 °C,

$AH_{45}Bt_5$ – 155 °C. The difference in the values of temperature transitions obtained by the DSC method and thermomechanical analysis is interpreted by the fundamental features of the methodological approaches to assessing the value of thermophysical indicators.

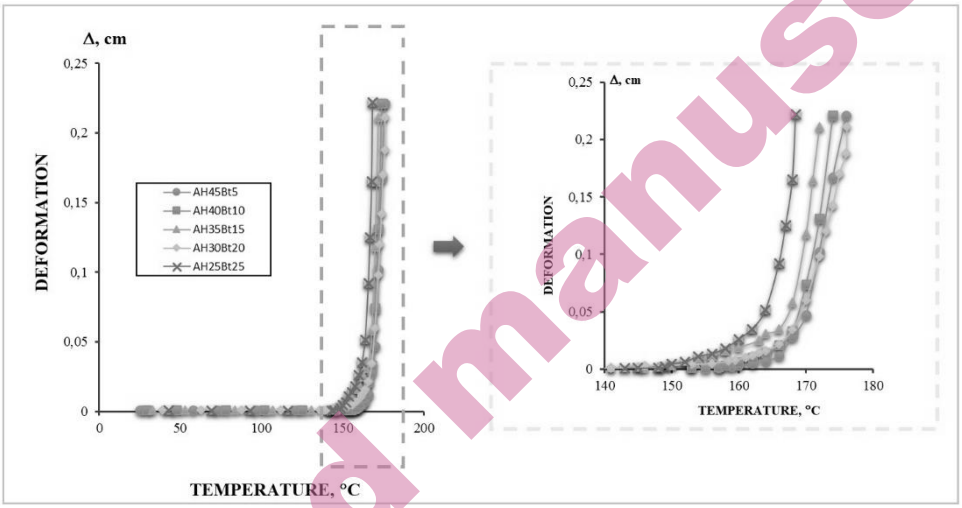

Fig. 6. Thermomechanical curves of the dependence of deformation on temperature for PP-R/PPC-*g*-MAH/$Al(OH)_3$/bentonite based polymer composites

Combustion tests were carried out in accordance with ASTM D3801. The figure 7 illustrates the results of a vertical burning flammability test performed on different polymer composite formulations over time.

As you can see from the figure 7, PP-R ignites quickly and burns intensely. By 30 seconds, a large flame is visible, and the polymer rapidly melts and drips onto the cotton. By 50 seconds, the sample is completely consumed, leaving the remaining time slots blank. By 80 seconds, the sample is entirely consumed and completely gone from the clamp, leaving nothing to record at 80 and 120 seconds. This indicates high flammability.

For $AH_{45}Bt_5$, flame spread is slower compared to pure PP-R. At 30 and 50 seconds, a char layer begins to form, reducing the dripping behavior.[24,25] The sample survives longer than pure PP-R, remaining clamped and burning slowly up to 80 seconds.

Increasing the bentonite filler to 25 wt % significantly improves performance. At 30 and 50 seconds, the vertical specimen sustains much less severe structural collapse. The additive creates a thick, protective carbonaceous char layer. This layer blocks oxygen and heat transfer, delaing total degradation past 80 seconds.

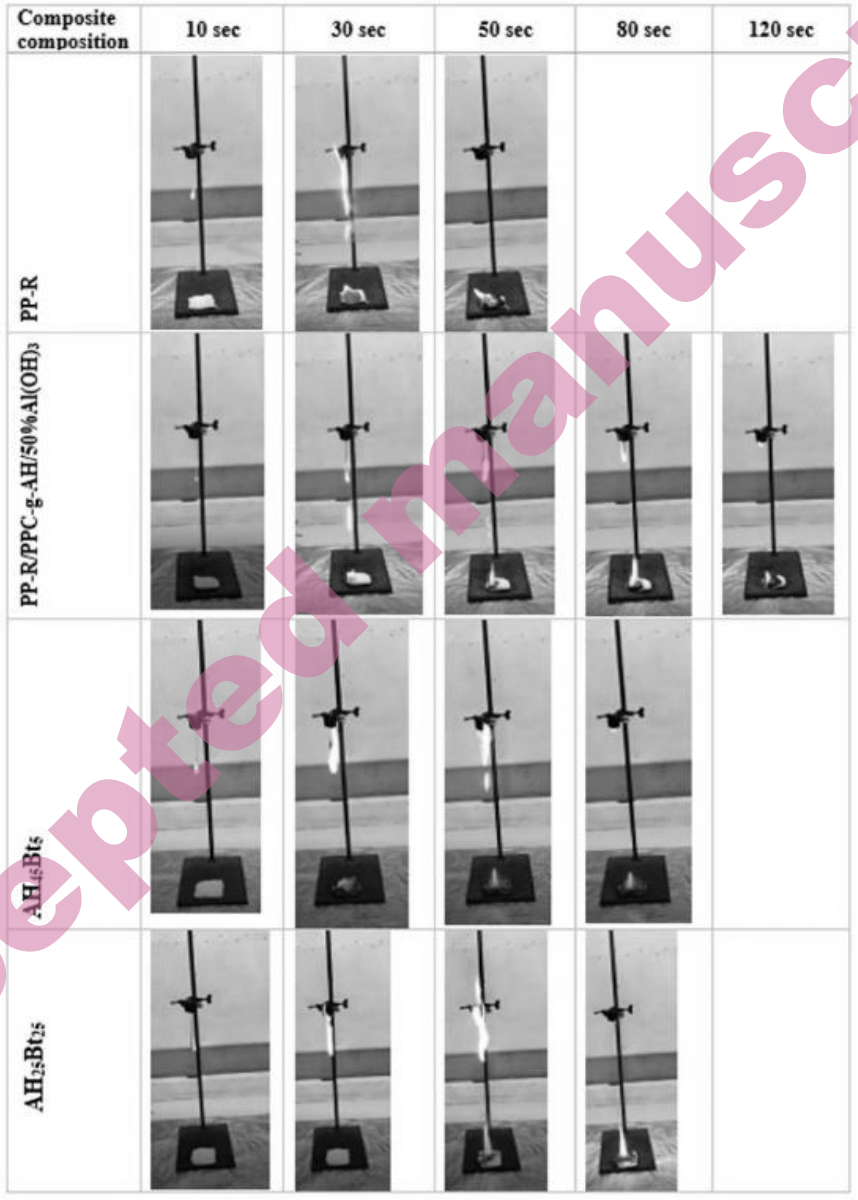

Fig. 7. Burning tests of PP-R and PP-R based composites

In samples containing bentonite, no burning droplets of the composite were released during combustion. Although the best result was obtained for the PP-R/PPC-*g*-AH/50 wt. %$Al(OH)_3$ sample, the samples filled with both fillers showed

better results than the original RPP (Fig. 7). As can be seen from the figure, while the original PP-R sample, which complies with the standard, burned for 50 seconds, the burning time of the samples to which both fillers were added increased to 80 seconds. Furthermore, unlike other samples, the sample with the addition of 25%$Al(OH)_3$/25% bentonite did not burn cotton within 30 seconds when the alloy was dropped. The figure demonstrates that adding flame retardant and synergistic additives / clays like bentonite significantly reduces the flame spread rate and dripping of the polymer.

CONCLUSION

The obtained composites were characterized using FTIR, SEM, physical-mechanical, TGA and DSC analyses. The effectiveness of modifying the composite with bentonite was assessed by changes in the physical and mechanical properties of the composite. Physical-mechanical studies have shown that the addition of bentonite clay to PP-R/$Al(OH)_3$ composites helps maintain melt fluidity even at high contents. DSC analysis revealed changes in the melting temperature of composite samples with different bentonite concentrations. The results showed that the inclusion of bentonite clay could effectively improve the thermal stability of PP-R/PPC-g-MAH/$Al(OH)_3$ composite. Thus, taking into account the results of the assessment of the physical and mechanical properties of polymer composites, it can be stated that the optimal content of bentonite in PP-R/PPC-g-MAH/$Al(OH)_3$/bentonite is 25%. The results of the conducted studies provide grounds for recommending this composite as a promising material with improved operational and environmental characteristics. Enhanced fire-rated PP-R is ideal for commercial hot / cold water, heating, and sprinkler system where flame retardancy is required.

И З В О Д

НАПРЕДНИ ПОЛИПРОПИЛЕНСКИ НАСУМИЧНИ КОПОЛИМЕРНИ НАНОКОМПОЗИТИ: УТИЦАЈ ПРИРОДНЕ БЕНТОНИТНЕ ГЛИНЕ И АЛУМИНИЈУМ-ХИДРОКСИДА НА МОРФОЛОГИЈУ И СВОЈСТВА

FATIMA MUSTAFAYEVA[1,2*], NAJAF KAKHRAMANOV[1]

[1]Institute of Polymer Materials of Ministry of Science and Education Republic of Azerbaijan, Sumgayit city, S. Vurgun Str. 124, AZ5004, Azerbaijan, and [2]Sumgayit State University, Sumgayit city, 43rd district, Baku street 1, AZ5008, Azerbaijan.

У раду се испитује утицај наночестица природног минерала бентонита и алуминијум-хидроксида на добијање нанокомпозита на бази компатибилизованог полипропиленског насумичног кополимера. Као компатибилизатор коришћен је насумични кополимер етилена и пропилена модификован анхидридом малеинске киселине. Укупна количина пунила у полипропиленском кополимеру била је 50 wt.%. Да би се проучио синергистички ефекат када се користи мешавина пунила, бентонит је укључен у формулацију у пет различитих концентрација (5, 10, 15, 20 и 25 wt.%). Композити су добијени механичким мешањем у растопу компатибилизоване полимерне матрице. Одређена су структурна,

морфолошка, физичко-механичка, термичка својства и отпорност на пожар добијених композитних материјала. Структурна и морфолошка својства су одређена коришћењем инфрацрвене спектроскопије (IR) и скенирајуће електронске микроскопије. На основу резултата IR спектроскопије и скенирајуће електронске микроскопије-енергетски дисперзивне рендгенске спектроскопије (SEM-EDX), потврђено је присуство елемената и веза које одговарају саставу бентонита и алуминијум-хидроксида, који су коришћени као пунила у саставу полипропиленског насумичног кополимера. Морфолошка студија открила је мање агломерате бентонитних наночестица. Термичка својства добијених композита одређена су термогравиметријском анализом и диференцијалном скенирајућом калориметријом. Термогравиметријска анализа показала је да додавање бентонита повећава термичку стабилност композита, о чему сведочи смањење брзине губитка масе. Механичка својства (затезна чврстоћа, издужење при прекиду) смањују се са повећањем концентрације бентонита. Синергистички ефекат добијен комбинованом употребом алуминијум-хидроксида и бентонита манифестовао се углавном у повећању мелт-индекса композита. Узорак који садржи 25 wt. % природног бентонита је показао највише вредности мелт-индекса до 3,12 g/10 min.

(Примљено 26. априла; ревидирано 20. јуна; прихваћено 23. јула 2026.)

REFERENCES

1. A. B. Mapossa, A. H. da Silva Júnior, C. R. S. de Oliveira, W. Mhike, *Polymers* **15(16)** (2023) 3443 (https://doi.org/10.3390/polym15163443)
2. F. A. Mustafayeva, N. T. Kakhramanov, N. S. Koseva, I. A. Ismayilov, *PPOR* **24(2)** (2023) 341-349 (https://doi.org/10.36719/1726-4685/94/341-349)
3. S. S. Ray, J. Tersur Orasugh, L. T. Temane, *Nanoclay-Containing Polymer Composites.* In: *Nanoclays.* Springer Series in Materials Science 350. (2025) Springer, Cham. (https://doi.org/10.1007/978-3-031-85304-3_4)
4. Y. Lei, X. Zhao, L. Xu, H. Li, J. Liang, G.H. Yeoh, W. Wang, *Fire* **7(9)** (2024) 308 (https://doi.org/10.3390/fire7090308)
5. N. V. Kostromina, Yu. V. Olikhova, V. S. Osipchik, *Bulletin of the Volgograd State Technical University.* **7(164)** (2015) 151-154. [In Russian]
6. İ. Karagöz, B. Ş. Şimşiroğlu, E. N. Özer, H. Sepetcioglu, J. Hızal, *J. Polym. Sci.* **63** (2025) 1505-1517 (https://doi.org/10.1002/pol.20240925)
7. J. L. Valin Rivera, C. R. Valenzuela Reyes, A. A. Quinteros Wachtendorff, A. Rodríguez Soto, M. Valin Fernández, R. Iquilio Abarzúa, A. González Ortega, G. García del Pino, F. R. Valenzuela Diaz, *Polymers* **15(19)** (2023) 3963. (https://doi.org/10.3390/polym15193963)
8. O. V. Alekseeva, A. V. Noskov, A. V. Agafonov, *Cellulose* **29** (2022) 3947–3961 (https://doi.org/10.1007/s10570-022-04546-1)
9. M. V. Fernández, J. L. V. Rivera, F. P. Rodríguez, H. F. Losada, M. E. F. Abreu, F. R. V. Diaz, A. R. Soto, A. A. Alvarez, R. Quinteros, C. G. Ketterer, G. G. del Pino, *Appl. Sci.* **13**(4) (2023) 2677 (https://doi.org/10.3390/app13042677)
10. R. Rothon, P. Hornsby, Chapter 9 - *Fire Retardant Fillers for Polymers.* Editor(s): C. D. Papaspyrides, P. Kiliaris. *Polymer Green Flame Retardants*, Elsevier (2014) 289-321. (https://doi.org/10.1016/B978-0-444-53808-6.00009-3)

11. F. A. Mustafayeva, N. T. Kakhramanov, *Chem-ChemTech [Izv. Vyssh. Uchebn. Zaved. Khim. Khim. Tekhnol.]*. **68(5)** (2025) 72-100 (https://doi.org/10.6060/ivkkt.20256805.7147)
12. A. P. Basnayake, J. P. Hidalgo, M. T. Heitzmann, *Const. Build. Mat.* **304** (2021) 124540 (https://doi.org/10.1016/j.conbuildmat.2021.124540)
13. F. A. Mustafayeva, N. T. Kakhramanov N. S. Koseva, *New Mat. Comp. Appl.* **4(1)** (2020) 28-37 (https://jomardpublishing.com/UploadFiles/Files/journals/NMCA/V4N1/MustafayevaF%20et%20al.pdf)
14. F. A. Mustafaeva, N. T. Kakhramanov, I. A. Ismailov, *Inorg. Mat. Appl. Res.* **13** (2022) 225-230 (https://doi.org/10.1134/S2075113322010282)
15. X. Yang, A. Shen, Y. Su, W. Zhao, *Construction and Building Materials*. **236** (2020) 117576, (https://doi.org/10.1016/j.conbuildmat.2019.117576)
16. X. Yang, A. Shen, M. Liang, Y. Jiang, Y. Meng, *Const. Build. Mat.* **309** (2021) 125077 (https://doi.org/10.1016/j.conbuildmat.2021.125077)
17. S. Kaleg, A. Budiman, A. Hapid, Amin, A. Muharam, Sudirja, D. Ariawan, K. Diharjo, *Int. J. Automot. Mechan. Eng.* **19** (2022) 9379-9390 (https://doi.org/10.15282/ijame.19.1.2022.02.0721)
18. B. A. Alshammari, A. M. Alenad, F. S. Al-Mubaddel, A. G. Alharbi, A. A. Al-shehri, H. A. Albalwi, F. M. Alsuabie, H. Fouad, A. I. Mourad, *Polymers* **14(16)** (2022) 3427 (https://doi.org/10.3390/polym14163427)
19. T. Almeida, A. Costa, R. Wellen, E. Canedo, L. Carvalho, *Mat. Res.* **20(6)** (2017) 1503-1510 (https://doi.org/10.1590/1980-5373-mr-2016-0577)
20. V. Zhorin, M. Kiselev, *Russian J. Phys. Chem. A* **95** (2021) 1307-1312 (https://doi.org/10.1134/S0036024421070311)
21. S. G. Karpova, A. Olkhov, A. Zhul'kina, A. Popov, A. Iordanskii, *Polym. Sci. Ser. A* **63** (2021) 369-381 (https://doi.org/10.1134/S0965545X21040040)
22. S .G. Karpova, A. A. Ol'khov, A. L. Iordanskii, S. M. Lomakin, N. S. Shilkina, A. A. Popov, K. Z. Gumargalieva, A. A. Berlin, *Polym. Sci. Ser. A* **58**, (2016) 76–86 (https://doi.org/10.1134/S0965545X16010041)
23. F. Mustafayeva, N. Kakhramanov, G. Martynova, N. Koseva, *J. Serb. Chem. Soc.* **90(6)** (2025) 789-802 (https://doi.org/10.2298/JSC241112021M)
24. F. Mustafayeva, N. Kakhramanov, Kh. Allahverdiyeva, T. Babayeva, N. Ashurova, *RSC Adv.* **16** (2026) 6257 (https://doi.org/10.1039/D5RA09525E)
25. Y. Lei, X. Zhao, L. Xu, H. Li, J. Liang, G.H. Yeoh, W. Wang, *Fire* **7** (2024) 308 (https://doi.org/10.3390/fire7090308).